Biology of Human Primary Bone Marrow Mesenchymal Stromal Stem Cells

Ghazanfari, Roshanak

2017

Cell PRESS
Open ACCESS

Cell Reports
Resource

Self-Renewing Human Bone Marrow Mesenspheres Promote Hematopoietic Stem Cell Expansion

Joan Isern,[1] Beatriz Martín-Antonio,[2] Roshanak Ghazanfari,[3] Ana M. Martín,[1] Juan A. López,[1] Raquel del Toro,[1] Abel Sánchez-Aguilera,[1] Lorena Arranz,[1] Daniel Martín-Pérez,[1] María Suárez-Lledó,[2] Pedro Marín,[2] Melissa Van Pel,[4] Willem E. Fibbe,[4] Jesús Vázquez,[1] Stefan Scheding,[3,5] Álvaro Urbano-Ispizúa,[2] and Simón Méndez-Ferrer[1,6,*]

[1]Centro Nacional de Investigaciones Cardiovasculares Carlos III, Madrid 28029, Spain
[2]Hematology Department, Hospital Clinic, University of Barcelona, IDIBAPS and Institute of Research Josep Carreras, Barcelona 08036, Spain
[3]Lund Stem Cell Center, University of Lund, 22184 Lund, Sweden
[4]Department of Immunohematology and Blood Transfusion, Leiden University Medical Center, Leiden 2333 ZA, The Netherlands
[5]Department of Hematology, Skåne University Hospital Lund, 22184 Lund, Sweden
[6]Department of Medicine, Icahn School of Medicine at Mount Sinai, New York, NY 10029, USA
*Correspondence: smendez@cnic.es
http://dx.doi.org/10.1016/j.celrep.2013.03.041

SUMMARY

Strategies for expanding hematopoietic stem cells (HSCs) include coculture with cells that recapitulate their natural microenvironment, such as bone marrow stromal stem/progenitor cells (BMSCs). Plastic-adherent BMSCs may be insufficient to preserve primitive HSCs. Here, we describe a method of isolating and culturing human BMSCs as nonadherent mesenchymal spheres. Human mesenspheres were derived from CD45$^-$ CD31$^-$ CD71$^-$ CD146$^+$ CD105$^+$ nestin$^+$ cells but could also be simply grown from fetal and adult BM CD45$^-$-enriched cells. Human mesenspheres robustly differentiated into mesenchymal lineages. In culture conditions where they displayed a relatively undifferentiated phenotype, with decreased adherence to plastic and increased self-renewal, they promoted enhanced expansion of cord blood CD34$^+$ cells through secreted soluble factors. Expanded HSCs were serially transplantable in immunodeficient mice and significantly increased long-term human hematopoietic engraftment. These results pave the way for culture techniques that preserve the self-renewal of human BMSCs and their ability to support functional HSCs.

INTRODUCTION

Hematopoietic stem cell (HSC) transplantation is routinely performed for lifesaving procedures in patients with hematologic malignancies or inherited metabolic/immune disorders. Different HSC sources, such as bone marrow (BM), peripheral blood, and cord blood, are used for allogeneic transplantation. The use of cord blood has recently been revived because of the scarcity of suitable BM donors and because cord blood is easily and non-invasively harvested, cryopreserved units are immediately available, and patients have a reduced risk of disease transmission and increased immune tolerance. However, the limited number of HSCs present in cord blood has restricted its use to low-body-weight recipients, whose survival correlates with HSC dose (Broxmeyer, 2011). Ex vivo expansion of cord blood HSCs would increase the number of patients who would benefit from this therapy and reduce their mortality risk. However, HSC expansion in culture remains challenging mainly due to our limited knowledge on the factors that drive HSC self-renewal. In vivo, this hallmark property of stem cells is maintained and regulated by a specific microenvironment referred to as "niche" (Schofield, 1978). Coculture of HSCs with stromal cells that recreate their natural niche is one of the current strategies aimed to expand cord blood HSCs. The cells that form the adult mammalian HSC niche and their specific functions in HSC maintenance are a subject of intense investigation (Mercier et al., 2012). Candidate HSC niche cells include BM stromal stem/progenitor cells (BMSCs; Méndez-Ferrer et al., 2010; Omatsu et al., 2010; Sacchetti et al., 2007), which have been proposed as a source of feeder cells for HSC culture. BMSCs are still today retrospectively isolated from primary human BM samples based on their high adherence to plastic and cultured from fibroblastic colony-forming units (CFU-F; Friedenstein et al., 1970). BMSCs cultured under standard conditions can support the ex vivo expansion of hematopoietic progenitors (Breems et al., 1997; Harvey and Dzierzak, 2004; Sharma et al., 2011; Verfaillie, 1992) but may be insufficient to preserve HSCs. To guarantee HSC engraftment in current clinical trials, a nonexpanded cord blood unit (or part of it) is being cotransplanted with an expanded one. The results reported to date indicate that the expanded cord blood unit initially contributes to hematopoiesis but only the nonexpanded cord blood unit is engrafted in the long term (de Lima et al., 2012), suggesting that cord blood CD34$^+$ cells that have expanded on BMSCs grown under standard conditions might not contain functional long-term HSCs. Alternatively, the relatively lower quantity of T lymphocytes present in the expanded unit might also compromise its engraftment (Urbano-Ispizua et al., 2001).

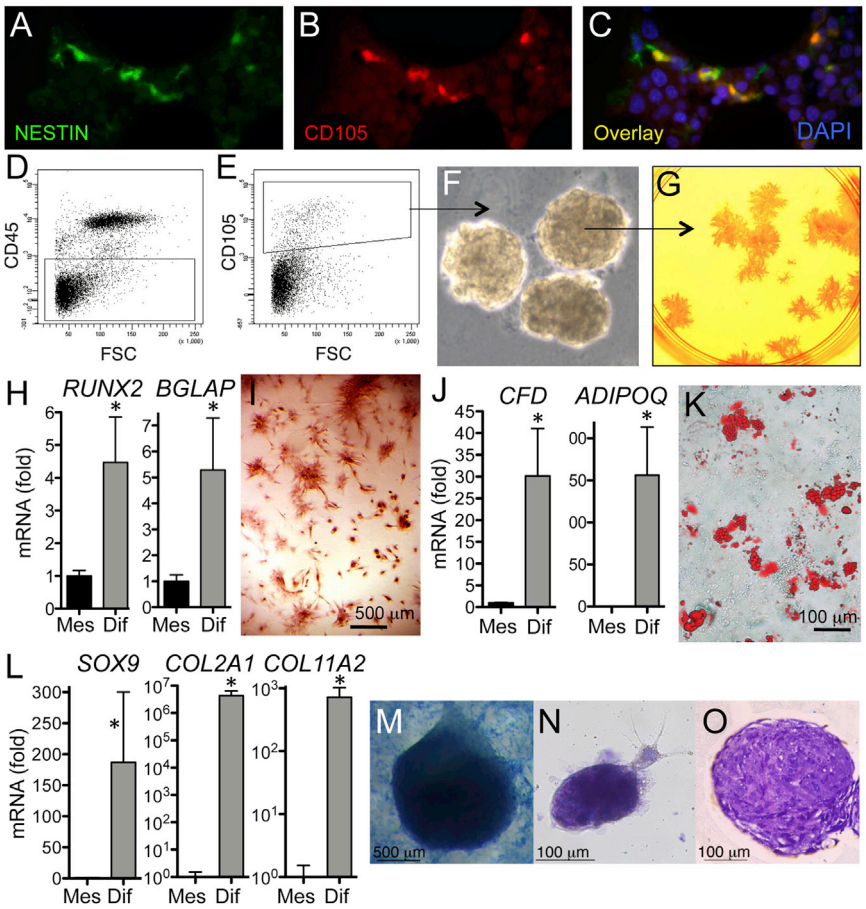

Figure 1. Human BM CD45$^-$ CD105$^+$ nestin$^+$ Cells Can Form Mesenspheres in Culture

Characterization of human BM mesensphere-forming cells.

(A–C) Coexpression of nestin and CD105/endoglin in a subset of human BM cells. Immunohistochemistry of healthy human BM biopsy showing expression of (A) NESTIN (green), (B) CD105 (red), and (C) composite image with nuclei counterstained with DAPI (blue).

(D–F) Human BM mesenspheres derived from CD45$^-$ CD105$^+$ cells.

(D and E) Representative flow diagrams showing the expression of (D) CD45 in BM nucleated cells and (E) CD105 in BM CD45$^-$ cells.

(F and G) Within human BM stroma, only CD105$^+$ cells could form mesenspheres (F), each of which yielded 175 ± 12 alkaline phosphatase$^+$ (pink) clonal adherent fibroblastic colonies (G).

(H–O) Multilineage differentiation of human BM mesenspheres into (H and I) osteoblasts, (J and K) adipocytes, and (L–O) chondrocytes. qPCR of genes associated with (H) osteoblastic (*RUNX2* and *BGLAP*), (J) adipogenic (*CFD* and *ADIPOQ*) and (L) chondrogenic (*SOX9*, *COL2A1*, and *COL11A2*) differentiation is shown in human BM mesenspheres (Mes) and their progeny cultured for 4 weeks in differentiation media (Dif; n = 3–22). *$p < 0.05$; unpaired two-tailed t test. Error bars indicate SEM.

(I, K, and M–O) Histological analyses show a fully differentiated phenotype of (I) alizarin red$^+$ osteoblasts, (K) oil red O$^+$ adipocytes, and (M) Alcian blue$^+$ or (N and O) toluidine blue$^+$ chondrocytes.

(O) Representative toluidine-blue-stained paraffin section of a sphere.

See also Figure S1.

Murine BMSCs can be isolated based on the expression of the intermediate filament protein nestin. Murine nestin$^+$ BMSCs can form clonal mesenchymal spheres (mesenspheres) that are able to self-renew and spontaneously differentiate into mesenchymal lineages both in vitro and in vivo. In the mouse, nestin$^+$ BMSCs are required to maintain HSCs in the BM and a single murine mesensphere is able to transfer hematopoietic activity to an ectopic bone ossicle (Méndez-Ferrer et al., 2010). Subendothelial nestin$^+$ cells have been reported in human BM (Ferraro et al., 2011). In this study, we aimed to characterize human BMSCs that are able to form mesenspheres, and assess their ability to support HSCs. Our results show that nestin$^+$ BMSCs with properties similar to those previously characterized in the mouse are present in human fetal and adult BM. When cultured and expanded in conditions that preserve their immature phenotype (i.e., as floating multipotent spheres), they can promote ex vivo human umbilical cord blood HSC expansion, which may potentially be of therapeutic use.

RESULTS

Human BM CD45$^-$ CD31$^-$ CD71$^-$ CD105$^+$ CD146$^+$ Cells Can Form Mesenspheres

We previously reported that in the BM of *Nestin-Gfp* transgenic mice (Mignone et al., 2004), CD45$^-$ GFP$^+$ cells contained all the CFU-F and had the capacity to form multipotent and self-renewing mesenspheres that spontaneously gave rise to mesenchymal lineages (Méndez-Ferrer et al., 2010). Because nestin is an intermediate filament protein with intracellular localization, we sought to identify candidate cell surface markers that would allow isolation of human BM nestin$^+$ cells. The transforming growth factor β (TGF-β) receptor III endoglin/CD105 is a glycoprotein that is expressed on the cell surface of osteoprogenitor cells (Aslan et al., 2006). We first examined endoglin expression in the BM of *Nestin-Gfp* transgenic mice and found that within CD45$^-$ CD31$^-$ Ter119$^-$ GFP$^+$ cells, the CD105$^+$ population displayed a higher sphere-forming efficiency as compared with CD105$^-$ cells (Figures S1A–S1C). Immunohistochemical analyses of human BM biopsies also showed CD105 expression in a subset of nestin$^+$ cells (Figures 1A–1C, S1D, and S1E). Therefore, we sorted human BM CD45$^-$ cells according to CD105 expression and found that CD45$^-$ CD105$^+$, but not CD45$^-$ CD105$^-$ cells, generated spheres (Figures 1D and 1E) that were mesenspheres, based on their high content of cells that were able to generate clonal alkaline phosphatase$^+$ fibroblastic colonies (Figure 1G) and robust multilineage differentiation into osteoblasts (Figures 1H and 1I), adipocytes (Figures 1J and 1K), and chondrocytes (Figures 1L–1O).

We characterized the immunophenotype of human BM mesensphere-initiating cells. In the human BM, CD45$^-$ CD31$^-$

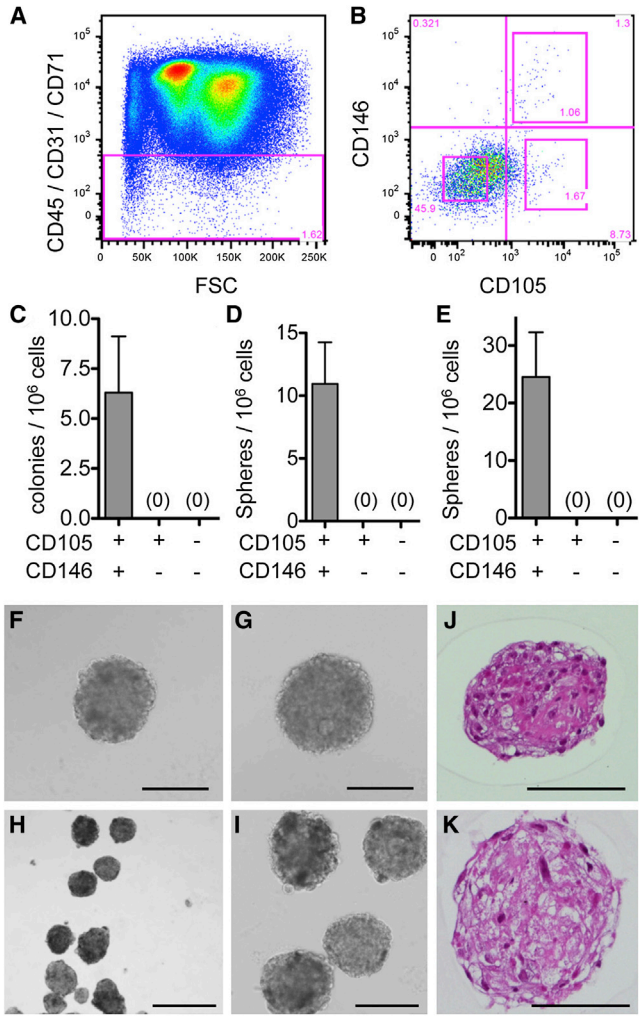

Figure 2. Human BM Mesenspheres Are Derived from CD45$^-$ CD31$^-$ CD71$^-$ CD105$^+$ CD146$^+$ Cells

(A and B) Immunophenotype of human BM mesensphere-forming cells. Healthy human BM CD45$^-$ CD31$^-$ CD71$^-$ cells (A) were sorted according to CD105 and CD146 expression into three populations (B).

(C–E) Frequency of (C) clonogenic fibroblastic colonies and (D and E) spheres derived from human BM nonhematopoietic/endothelial/erythroid CD105$^+$ CD146$^+$, CD105$^+$ CD146$^-$, and CD105$^-$ CD146$^-$ cells plated (C and D) at clonal density or (E) by single-cell deposition. The frequency is related to BM mononuclear cells after separation with the RosetteSep Kit (StemCell Technologies) (n = 3 donors; error bars indicate SEM).

(F–I) Representative examples of human BM mesenspheres obtained by (F and G) single-cell deposition or (H and I) bulk culture at low density.

(J and K) Histology of H&E-stained paraffin sections of human BM mesenspheres.

Scale bars, 200 μm (F, G, and I), 500 μm (H), and 100 μm (J and K). See also Figure S2.

CD146$^{+/low}$ cells have been reported to contain all CFU-F (Sacchetti et al., 2007; Tormin et al., 2011). Hence, CD45$^-$ CD31$^-$ CD71$^-$ (nonhematopoietic/endothelial/erythroid) cells were sorted according to CD146 and CD105 expression (Figures 2A, 2B, and S2), and compared in terms of their capacity to form clonogenic fibroblastic colonies and mesenspheres at clonal density. All clonogenic and sphere-forming capacities were restricted to the CD105$^+$ CD146$^+$ subset, and CD105$^-$ CD146$^-$ and CD105$^+$ CD146$^-$ cells did not generate any progeny. The frequency of clonogenic fibroblastic colonies (3.4% ± 2.1%) was close to the sphere-forming efficiency (5.9% ± 2.3%) obtained from CD45$^-$ CD31$^-$ CD71$^-$ CD105$^+$ CD146$^+$ cells plated at low density. Sphere-forming efficiency (12.8% ± 4.7%) was doubled when CD45$^-$ CD31$^-$ CD71$^-$ CD105$^+$ CD146$^+$ cells were plated by single-cell deposition (Figures 2C–2I). The spheres showed a compact structure with a thick core containing fibroblastic-shaped cells embedded in a dense eosinophilic extracellular matrix (Figures 2J and 2K).

We next addressed whether human mesenspheres could be obtained from fetal BM and whether these specific culture conditions could select for the growth of sphere-forming cells without the need for multiple selection markers. Fetal human BM mononuclear cells were immunomagnetically depleted of CD45$^+$ cells and plated in mesensphere medium. Numerous human primary spheres formed after 7–10 days in culture (Figure 3A) and expressed not only *NESTIN* but also high messenger RNA (mRNA) levels of stem cell factor (*KITL*) and leptin receptor (*LEPR*; Figure 3B), which was recently shown in the mouse to mark KITL-producing BMSCs that critically support HSCs (Ding et al., 2012). Fetal human BM mesenspheres were capable of robustly differentiating into osteoblasts (Figures 3C and 3D), adipocytes (Figures 3E and 3F), and chondrocytes (Figures 3G and 3H), providing further proof of their BMSC origin.

These results indicate that culture conditions similar to those previously optimized in the mouse (Méndez-Ferrer et al., 2010) can promote the selective growth of human mesenspheres from fetal and adult BM stromal (immunomagnetically enriched) CD45$^-$ cells without the need for additional selection markers, although, in the adult human BM, mesensphere-initiating cells are highly enriched within the CD45$^-$ CD31$^-$ CD71$^-$ CD105$^+$ CD146$^+$ cell population.

Expansion of Undifferentiated Human BM Mesenspheres

Adult human BM mesenspheres were grown and expanded under two different culture conditions, i.e., in cytokine-enriched medium containing either human serum (HS) or chicken embryo extract (CEE, a culture supplement that stimulates stem cell self-renewal; Stemple and Anderson, 1992). The CEE mesenspheres were relatively undifferentiated compared with the HS mesenspheres, as shown by increased *NESTIN* expression and reduced mRNA levels of genes required for osteoblastic and adipocytic differentiation (Figure 4A). The spheres could be serially expanded under both culture conditions, although the CEE mesenspheres generated more spheres over serial passages (Figure 4B; 550 versus 320 spheres at passage 3). In addition, whereas the CEE mesenspheres remained in suspension and morphologically identical over >2 months in culture (Figure 4C), the HS spheres attached even to ultralow-adherence dishes and disappeared in the long term as a result of cell outgrowth from the spheres as an adherent monolayer (Figure 4D). Expanded CEE mesensphere-forming cells maintained expression of CD105 and CD146 (17% of sphere-forming cells; Figure 4E) and did not express CD45, CD31, or CD71 (data not

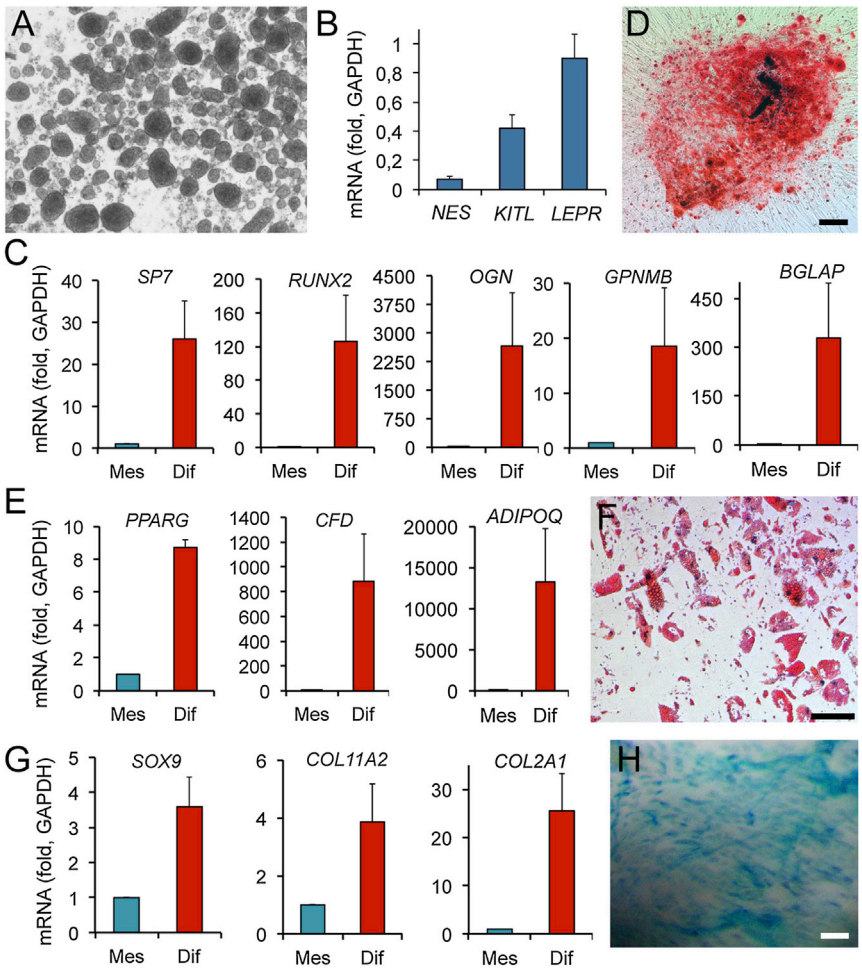

Figure 3. Human Mesenspheres Can Be Derived from Fetal BM

(A) Representative spheres from immunomagnetically enriched fetal human BM CD45$^-$ cells.

(B) Fetal human BM mesenspheres express *NESTIN*, stem cell factor (*KITL*), and leptin receptor (*LEPR*) mRNA; qPCR, n = 3.

(C–H) Multilineage differentiation of fetal human BM mesenspheres. Spheres were enzymatically dissociated and cultured for 3 weeks in (C and D) osteoblastic, (E and F) adipocytic, and (G and H) chondrocytic differentiation media.

(C, E, and G) qPCR of genes associated with (C) osteoblastic (osterix, *SP7*; osteoglycin, *OGN*; Runt-related transcription factor 2, *RUNX2*; osteoactivin, *GPNMB*; osteocalcin, *BGLAP*), (E) adipogenic (peroxisome proliferator-activated receptor gamma, *PPARG*; adipsin, *CFD*; adiponectin, *ADIPOQ*), and (G) chondrogenic (sex determining region Y-box 9, *SOX9*; collagen 11α2, *COL11A2*; collagen 2α1, *COL2A1*) differentiation (n = 3). Error bars in (B), (C), (E), and (G) indicate SEM.

(D, F, and H) Histological analyses showing a differentiated phenotype of (D) alizarin red$^+$ osteoblasts, (F) oil red O$^+$ adipocytes, and (H) Alcian blue$^+$ chondrocytes. Scale bar, 100 μm.

shown). After being digested and replated three times, more than half of the CEE mesenspheres differentiated into osteoblasts and adipocytes, and all of the spheres that were analyzed (n = 20) differentiated into toluidine blue$^+$ chondrocytes (data not shown), indicating preservation of multipotency under these culture conditions (Figure 4F). To test whether human mesenspheres were capable of in vivo maintenance and hematopoietic support, single primary spheres were allowed to attach onto phosphocalcic ceramic ossicles and then implanted subcutaneously in immunodeficient mice, as previously described (Méndez-Ferrer et al., 2010). Ossicles were harvested after 2 months and enzymatically digested, and the recovered cells were isolated by fluorescence-activated cell sorting (FACS) according to expression of mCD45, hCD146, and hCD105, and subcultured at clonal density in mesensphere-forming medium (Figures S3A and S3B). The sphere-forming efficiency of hCD105$^+$/hCD146$^+$ cells (21% ± 8%) was 80-fold higher than that of hCD105$^-$ hCD146$^-$ cells (0.3% ± 0.2%) recovered from the ossicles (Figure S3C). Altogether, these results indicate preserved multipotency and maintenance of human BMSCs grown as mesenspheres.

We performed a quantitative proteomics analysis of the supernatants of CEE and HS spheres to identify the most abundant proteins that were differentially produced by human BMSCs under both conditions. The quantified proteins were subjected to a systems biology comparative analysis. HS mesenspheres displayed higher expression of proteins involved in metabolic processes, gene expression and translation, mitochondrial and nucleolar function, and ribonucleoprotein complex and actin cytoskeleton formation. In contrast, CEE mesenspheres produced more proteins involved in cell adhesion, collagen and basement membrane production, extracellular matrix-protein interaction, axon guidance, response to hypoxia, wounding, and organic cyclic compound production (Figure 4G). CEE mesenspheres also produced more proteins involved in angiogenesis, secretory granule production, and signal transduction, as well as more glycosylated and plasma integral proteins. Interestingly, HS sphere-derived secretome contained more proteins involved in cell-cycle progression, whereas CEE mesenspheres expressed more proteins involved in cell-cycle arrest, such as those involved in TGF-β signaling (Figure 4H; Table S1). These results indicate that nonadherent human mesenspheres are qualitatively distinct but may change their phenotype upon adherence to plastic. When cultured in conditions that reduce their attachment to the dish, they display reduced proliferation and metabolic rate, but increased maintenance and production of active molecules as compared with more-differentiated BMSCs that exhibit increased adhesion to plastic.

Human BM Mesenspheres Support HSCs

Our previous studies indicated that undifferentiated nestin$^+$ BMSCs have essential functions in the regulation of murine

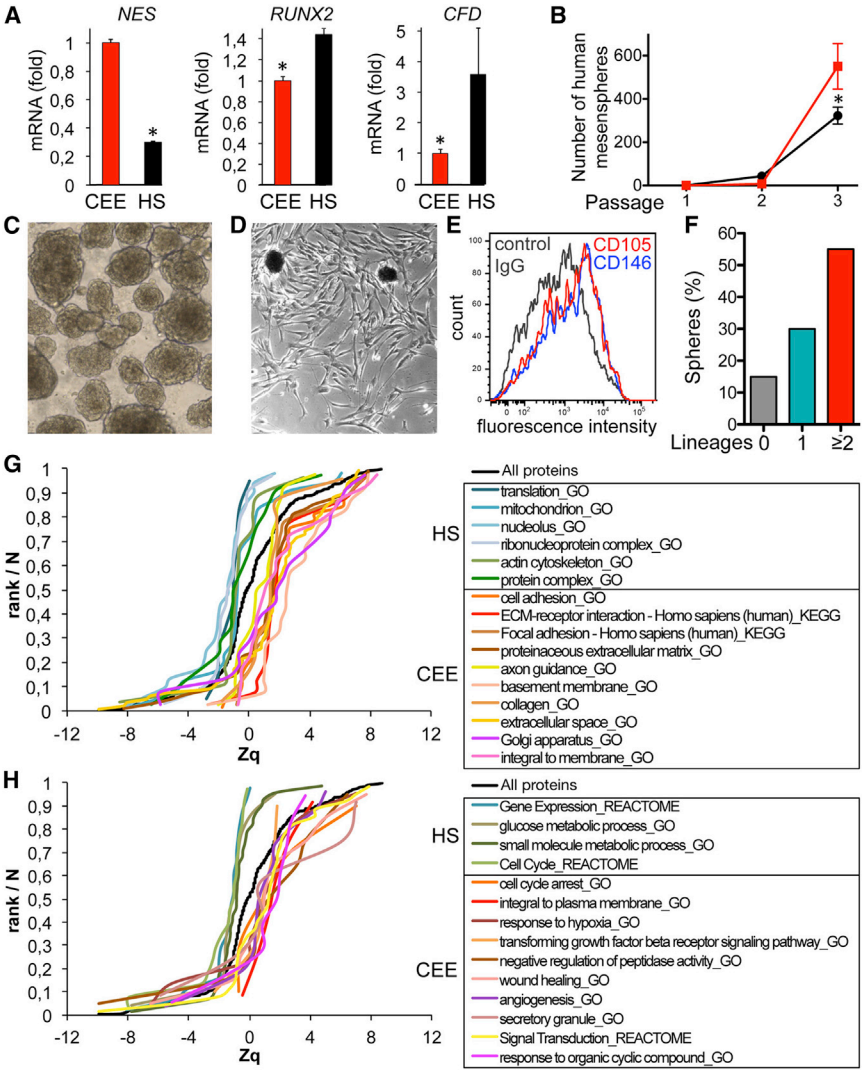

Figure 4. Expansion of Self-Renewing Human BM Mesenspheres

(A) qPCR analyses of the expression of nestin (*NES*) or differentiation markers (*RUNX2* and *CFD*) in human BM mesenspheres cultured with CEE (red) or HS (black), normalized to GAPDH.

(B–F) In vitro self-renewal of human mesenspheres, showing the number of CEE (red) and HS (black) BM spheres over three passages. *$p < 0.05$; unpaired two-tailed t test; error bars indicate SEM.

(C and D) CEE mesenspheres (C) were preserved over passages, in contrast to HS spheres (D), which attached even to ultralow-adherence plastic.

(E) Representative FACS histograms of CEE mesenspheres expanded over four passages, which remained $CD105^+$ (red) and $CD146^+$ (blue); gray, control isotype staining.

(F) After three passages, 55% of mesenspheres (11/20) differentiated into two or more mesenchymal lineages.

(G and H) Comparison of the secretome of CEE and HS mesenspheres by quantitative proteomics. The cumulative frequency distributions of standardized $\log_2$ ratios (Zq) of proteins grouped into ontological categories from GO, KEGG, or REACTOME databases show the coordinated increase or decrease of proteins belonging to these categories. Related ontological categories have been conventionally distributed into two graphs to facilitate viewing of the pathways enriched in CEE (Zq > 0, right shift of sigmoidal curves) or HS (Zq < 0, left shift of curves) spheres when compared with the predicted cumulative normality plot of the standardized variable at the protein level for all proteins (black curves).

See also Figure S3 and Table S1.

HSCs (Méndez-Ferrer et al., 2010). Therefore, we studied whether culture conditions that better preserve BMSC self-renewal could also enhance their support of HSCs. Coculture of ~100 fresh CEE mesenspheres with 2×10^5 cord-blood-derived $CD34^+$ cells did not exceed the cell expansion achieved only with cytokines, but doubled the number of primitive hematopoietic progenitors, as measured using the long-term culture-initiating cell assay (LTCIC; Figure S4A), suggesting that human BM mesenspheres could sustain cord blood HSC self-renewal. Indeed, the frequency of cord-blood-derived HSCs, defined as $CD34^+$ $CD38^-$ $CD49f^+$ cells (Notta et al., 2011), was already increased 3 days after coculture with human BM mesenspheres (Figure S4B).

Immature Human BM Mesenspheres Expand Multipotent and Long-Term Engrafting Cord Blood HSCs

We directly compared the ability of undifferentiated (CEE) and more-differentiated (HS) mesenspheres to expand functional HSCs capable of engrafting into immunodeficient mice. Cord blood $CD34^+$ cells were cultured alone with cytokines or in the presence of expanded HS or CEE adult BM mesenspheres (Figure 5A). The HS and CEE mesenspheres respectively yielded a 6- and 40-fold expansion of cord blood $CD34^+$ cells as compared with the control medium (Figures 5B, 5C, and S5A). The capacity of cultured human $CD34^+$ cells to contribute to hematopoiesis was tested by transplantation into immunodeficient mice. Cord blood $CD34^+$ cells expanded in coculture with HS mesenspheres did not increase the presence of human $CD45/CD71^+$ hematopoietic cells in the BM of NOD/SCID mice when compared with $CD34^+$ cells cultured only with cytokines. In contrast, cord blood $CD34^+$ cells expanded in coculture with CEE mesenspheres yielded a 38-fold increase in BM human hematopoietic chimerism of NOD/SCID mice 2 months later (average 6.1% engraftment; Figures 5D and S5B). In addition, subcutaneous implantation of 2×10^6 cocultured hematopoietic cells did not generate teratomas in NOD/SCID mice (data not shown).

We tested the self-renewal and multilineage differentiation potential of expanded HSCs by transplantation into NOD/SCID/gamma (NSG) mice. Two months after transplantation into NSG mice, cord blood $CD34^+$ cells expanded in coculture with

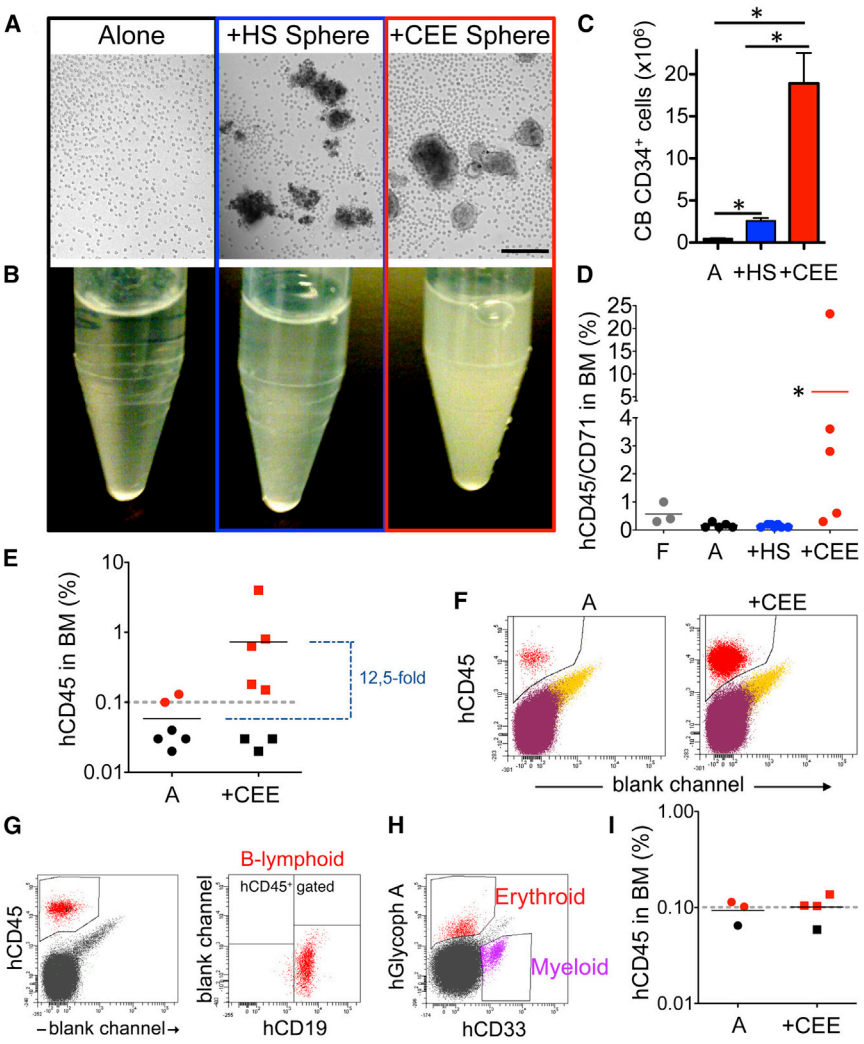

Figure 5. Increased HSC Engraftment in Immunodeficient Mice from Cord Blood CD34$^+$ Cells Cocultured with Primitive Human BM Mesenspheres

(A) Cord blood CD34$^+$ cells were cultured in serum-free medium containing cytokines in the absence (Alone, black) or presence of human BM mesenspheres previously expanded with HS (blue) or CEE (red).

(B and C) HS and CEE mesenspheres previously expanded over 4 weeks respectively yielded 6- and 40-fold expansion of cord blood CD34$^+$ cells as compared with CD34$^+$ cells cultured alone (A).

(C) Number of cord blood CD34$^+$ cells measured by FACS after 16 days of culture (n = 3).

(D–I) CEE mesenspheres can expand human HSCs that are capable of multilineage reconstitution and serial engraftment in immunodeficient mice.

(D) Percentage of human CD45$^+$/CD71$^+$ cells in the BM of NOD/SCID mice 2 months after transplantation of 10^4 freshly thawed (F) cord blood CD34$^+$ cells or their progeny after 16 days of culture with cytokine-supplemented serum-free medium alone (A) or in the presence of HS (+HS) or CEE (+CEE) spheres; n = 3; *p < 0.05; unpaired two-tailed t test. Error bars indicate SEM.

(E) Percentage of human CD45$^+$ cells in the BM of NSG mice 2 months after transplantation of the progeny of nonfrozen 10^4 cord blood CD34$^+$ cells cultured for 2 weeks in cytokine-supplemented serum-free medium alone (A) or in the presence of CEE (+CEE) spheres.

(F) Representative FACS diagrams of hCD45-stained BM cells from NSG mice transplanted with CD34$^+$ cells that were cultured alone (A) or in the presence of CEE (+CEE) spheres.

(G and H) Multilineage differentiation of cord blood CD34$^+$ cells in NSG mice. Representative FACS diagrams of BM cells 2 months after transplantation of cultured cord blood CD34$^+$ cells in NSG mice. BM cells were stained with (G) anti-hCD45 (hematopoietic) and anti-hCD19 (B-lymphoid) or with (H) anti-hCD33 (myeloid) and anti-hCD235a/glycophorin A (erythroid) antibodies.

(I) Serial reconstitution of expanded cord blood CD34$^+$ cells in NSG mice. Secondary transplant of BM cells harvested from mice that showed a similar hCD45 engraftment 2 months after transplantation of CD34$^+$ cells that were cultured alone (A) or in the presence of CEE (+CEE) spheres.

(E and I) Following previous studies, engraftment was considered positive (red dots) when $\geq$0.1% hCD45 cells were engrafted (gray dotted line) and negative (black dots) below this threshold.

See also Figures S4 and S5, and Table S2.

CEE mesenspheres yielded a 12.5-fold increase in human hematopoietic chimerism of NSG BM when compared with CD34$^+$ cells cultured only with cytokines. Although only 40% of mice (2/5) transplanted with CD34$^+$ cells cultured alone showed human hematopoietic engraftment above the 0.1% threshold, 62.5% (5/8) showed engraftment of CD34$^+$ cells that had been cocultured with CEE mesenspheres (Figures 5E and 5F). Expanded cord blood CD34$^+$ cells contained functional HSCs capable of accomplishing multilineage differentiation into B-lymphoid (Figure 5G), myeloid, and erythroid cells (Figure 5H). We tested the capacity of cultured HSCs to engraft into secondary recipient mice. BM cells from mice that showed a similar hCD45 engraftment after transplantation of CD34$^+$ cells cultured alone or in the presence of CEE spheres were used for secondary transplants. The BM engraftment of hCD45$^+$ cells 2 months after secondary transplantation demonstrates that expanded cord blood CD34$^+$ cells that yielded a similar engraftment in primary recipients were equally able to reconstitute secondary recipient mice (Figure 5I).

Human BM Mesenspheres Expand Long-Term Cord Blood HSCs through Soluble Secreted Factors

Although some studies have suggested that cell contact between BMSCs and hematopoietic progenitors is required to expand the latter (Harvey and Dzierzak, 2004; Kawada et al., 1999; Thiemann et al., 1998), other studies have shown an effect that is largely independent of direct cell contact (Breems et al., 1997; Verfaillie, 1992). We tested the capacity of expanded human mesenspheres to support cord blood CD34$^+$ cells in direct coculture or separated by transwell. A similar expansion of cord

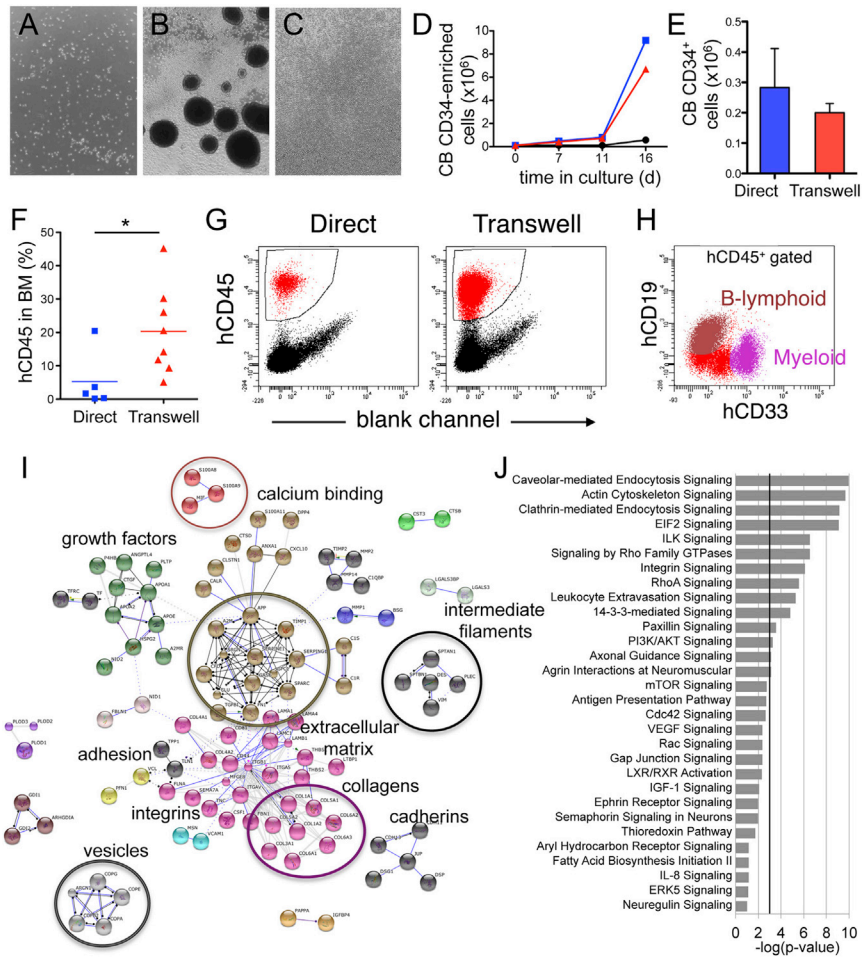

Figure 6. Human BM Mesenspheres Support Cord Blood HSCs Mainly through Secreted Factors

(A–C) Cord blood CD34$^+$ cells were cultured for 16 days in serum-free medium containing cytokines (A) in the absence of or (B and C) in coculture with human fetal mesenspheres, either (B) in direct contact or (C) separated by transwell.

(D) Growth curve of cord blood CD34-enriched cells cultured alone (black line), in contact with human mesenspheres (blue line) or separated from them by transwell (red line).

(E) Number of CD34$^+$ cells measured by FACS (n = 3; error bars indicate SEM).

(F–H) Soluble secreted factors produced by human BM mesenspheres expand cord blood HSCs capable of long-term reconstitution and multilineage differentiation in immunodeficient mice.

(F) Percentage of human CD45$^+$ cells in the BM of NSG mice 16 weeks after transplantation of cord blood CD34$^+$ cells cultured for 3 weeks with human BM mesenspheres in direct contact or separated by transwell. *p < 0.05; unpaired two-tailed t test.

(G) Representative FACS diagrams of hCD45-stained BM cells from NSG mice 4 months after transplantation of CD34$^+$ cells cultured in both conditions.

(H) Representative FACS diagram showing long-term multilineage reconstitution. BM cells were stained with anti-hCD45 (hematopoietic), anti-hCD19 (B-lymphoid), and anti-hCD33 (myeloid) antibodies.

(I) Protein-protein interactions predicted from the list of proteins detected in the secretome of human CEE BM mesenspheres (n = 3 independent donors). Only proteins for which two or more peptides were detected in two or more samples were considered for the analyses using STRING 9.0. Interactions were identified from experimental data and databases using a high confidence level (0.700). The clustering was performed using the MCL algorithm (inflation parameter set at 2).

(J) Enrichment in relevant canonical pathways detected using Ingenuity Pathway Analysis.

See also Figures S4 and S5.

blood CD34$^+$ cells was detected in the direct and transwell cocultures with CEE mesenspheres (Figures 6A–6E), suggesting that soluble factors secreted by the spheres might be sufficient to promote HSC expansion. We compared the direct and transwell cocultures in terms of their capacity to expand cord blood HSCs with long-term engraftment in immunodeficient mice. Cord blood CD34$^+$ cells that had been cocultured for 3 weeks with human mesenspheres, either directly or separated by transwell, were i.v. transplanted into NSG mice. Strikingly, a 4-fold higher human hematopoietic chimerism was detected 16 weeks later in the BM of mice transplanted with cord blood cells that had been cocultured using transwell as compared with direct coculture. Notably, human chimerism was >20% in 50% of mice from the transwell group (Figures 6F and 6G). Long-term engraftment from cocultured cord blood HSCs was also associated with multilineage reconstitution (Figure 6H). These results indicated that soluble factors secreted from human BM mesenspheres are responsible for HSC expansion. Therefore, we performed high-throughput mass spectrometry analyses of proteins secreted by CEE human mesenspheres to better characterize CEE-mesensphere-forming cells and candidate HSC-supporting factors. These analyses identified >1,100 proteins in three independent samples. Potentially secreted proteins were determined and quantitated as previously described (Bonzon-Kulichenko et al., 2011). Proteins of the TGF-β pathway that, similarly to some of their target genes (e.g., osteopontin), have been reported to induce HSC quiescence (Larsson and Karlsson, 2005; Nilsson et al., 2005; Stier et al., 2005) were also detected. Growth factors such as hepatocyte, basic fibroblastic and connective tissue growth factors, and other molecules that have been shown to support HSCs, such as insulin-like growth factor (IGF), angiopoietin-like growth factor (Zhang et al., 2008), and prostaglandin-related proteins (Goessling et al., 2011; Hoggatt et al., 2009; North et al., 2007), were also detected and may represent other candidate factors that support HSCs. The most abundant secreted proteins were those involved in basement membrane and extracellular matrix formation, such as collagens, laminins, fibronectin, proteoglycans, nidogens,

and matrix metalloproteinases. Integrins and other related proteins, such as vinculin and talin, were also abundant. Different calcium transport and metabolism proteins, as well as neural guidance/outgrowth and norepinephrine catabolism proteins, were also detected. The BMSC markers found in these samples included endoglin, CD90, CD276, VCAM-1, CD44, and CD151. Filament proteins associated with nestin, such as vimentin, desmin, plectin, and filamin-A, were abundant in these samples (Figures 6I and 6J; Table S2). These results show that human BM mesenspheres secrete many different proteins that are able to affect HSC function, and suggest that most likely multiple factors secreted by them contribute to maintain HSCs in culture.

In summary, this study demonstrates that BMSCs with features similar to those previously characterized in the mouse (Méndez-Ferrer et al., 2010) are present in human fetal and adult BM. When expanded in novel nonadherent conditions that preserve their immature phenotype, they can promote ex vivo HSC self-renewal and expansion, which may potentially be of therapeutic use.

DISCUSSION

We describe here a method of isolating and culturing human BMSCs in a way that better preserves their self-renewal and HSC niche functions. Over the past few years, different strategies have been used for ex vivo expansion of HSCs, especially those derived from cord blood. These include treatments with angiopoietin-like proteins, IGF-binding protein 2 (Zhang et al., 2008), the Notch ligand Delta1 (Delaney et al., 2010), antagonists of the aryl hydrocarbon receptor (Boitano et al., 2010), dimethylprostaglandin E2 (Goessling et al., 2011; Hoggatt et al., 2009; North et al., 2007), and inhibitors of apoptotic proteases (Sangeetha et al., 2010). BM engraftment of cord blood HSCs is also accelerated after inhibition of CD26/dipeptidylpeptidase IV (Campbell et al., 2007; Christopherson et al., 2007) and ex vivo fucosylation (Robinson et al., 2012).

BMSCs cultured under standard adherent conditions have been shown to support the ex vivo expansion of hematopoietic progenitors (Breems et al., 1997; Harvey and Dzierzak, 2004; Sharma et al., 2011; Verfaillie, 1992) but may be insufficient to preserve primitive HSCs (de Lima et al., 2012). However, BMSCs are still retrospectively isolated based on their high plastic adherence and/or cultured in minimal medium supplemented with serum.

We previously showed that self-renewing murine mesenspheres are able to transfer hematopoietic activity to an engineered bone scaffold (Méndez-Ferrer et al., 2010). In the current study, we characterized a human BM cell population that was able to form mesenspheres, and assessed its capacity to support cord blood HSCs. Our results demonstrate that nestin$^+$ BMSCs with properties similar to those previously characterized in the mouse are present in human fetal and adult BM. We did not need to use specific surface markers to grow human mesenspheres, because we could simply derive them from immunomagnetically enriched CD45$^-$ cells using a specific culture medium. Like colony-initiating cells (CFU-F), mesensphere-forming cells were highly enriched in the CD45$^-$ CD31$^-$ CD71$^-$ CD105$^+$ CD146$^+$ population. A subset of the cells contained in the spheres remained CD105$^+$ and CD146$^+$ over passages.

Although only a small number of primary mesenspheres could be obtained from human BM aspirates, they could be propagated over 2 months during multiple divisions. Notably, spheres cultured with CEE showed increased in vitro self-renewal as compared with those cultured with HS. Moreover, the presence of HS instead of CEE in the medium led to reduced nestin expression, upregulation of differentiation markers, and cell attachment, even to ultralow-adherent plastic. In agreement with this, other studies have suggested that nonadherent human BM mesenchymal progenitors display a higher differentiation potential (Baksh et al., 2003) and cannot be maintained with serum (Di Maggio et al., 2012). These changes were associated with a marked difference in HSC support. Although coculture with HS spheres increased the cord blood CD34$^+$ cell yield, only CEE spheres could increase the engraftment in immunodeficient mice.

Notably, cord blood HSC expansion was triggered by soluble secreted factors produced by CEE mesenspheres. Although some studies have suggested that cell contact between BMSCs and hematopoietic progenitors is required to expand the latter (Harvey and Dzierzak, 2004; Kawada et al., 1999; Thiemann et al., 1998), other studies have suggested that direct cell-cell interaction is not required (Breems et al., 1997; Verfaillie, 1992). Our results support the last contention, since a 4-fold higher long-term reconstitution was detected from cord blood cells cocultured with human mesenspheres that were separated by transwell. This was also associated with a higher recovery of mesenspheres cocultured on the transwell compared with those directly cocultured using ultralow-adherent plastic dishes (data not shown). Since the coculture medium in all cases was a hematopoietic-supporting medium rather than a mesensphere medium, these differences suggest that the mere attachment of the spheres to the plastic dish during the direct coculture changed their phenotype and impaired their ability to secrete factors capable of expanding HSCs.

Candidate factors that were abundantly produced by CEE spheres and could contribute to HSC expansion include proteins of the TGF-β pathway that have been reported to preserve HSC quiescence (Larsson and Karlsson, 2005; Nilsson et al., 2005; Stier et al., 2005); hepatocyte, basic fibroblastic and connective tissue growth factors, IGF, and angiopoietin-like growth factor (Zhang et al., 2008); and prostaglandin-related proteins (Goessling et al., 2011; Hoggatt et al., 2009; North et al., 2007). Therefore, multiple factors could contribute to the enhanced HSC support displayed by CEE mesenspheres. Elucidation of critical mediators in the future might facilitate the optimization of chemically defined media for human HSC expansion. The ability to expand cord blood HSCs in transwell coculture with human mesenspheres might increase their safety in humans and facilitate testing of their potential clinical benefit. In addition, cells that expanded under these conditions did not generate teratomas in immunodeficient mice.

In summary, these results demonstrate that primitive nestin$^+$ BMSCs are present in human fetal and adult BM. Without the need for complex isolation protocols, they can give rise to self-renewing mesenspheres with a more primitive phenotype and enhanced ex vivo HSC support as compared with more-differentiated BMSCs. These studies pave the way for new isolation and culture strategies to better preserve the self-renewal of human

BMSCs and their ability to support HSCs, which will critically determine the success of these approaches in the clinical arena.

EXPERIMENTAL PROCEDURES

Mouse Strains

NOD.CB17-Prkdc^{scid}/J, NOD/LtSz-scidIL2Rg^{null} (Jackson Laboratories) and *Nestin-Gfp* (Mignone et al., 2004) transgenic mice were used in these studies. Experimental procedures were approved by the Animal Care and Use Committee of the Spanish National Center for Cardiovascular Research.

Cell Isolation and Culture

BM aspirates were obtained in the Hospital Clínic (University of Barcelona, Spain) and Skåne University Hospital (Lund, Sweden) with written consent from healthy individuals, donors of BM hematopoietic progenitor cells for allogeneic transplantation or patients free of hematological diseases. The samples obtained were processed in two different ways. For sorting experiments, human BM mononuclear cells were enriched from 60 ml human BM aspirates using the RosetteSep kit (StemCell Technologies). Cells were stained with 7-Aminoactinomycin D (7AAD) solution (Sigma) and the following mouse anti-human antibodies (BD PharMingen): CD31-FITC (clone WM59), CD45-FITC (clone 2D1), CD71-FITC (clone M-A712), CD105-APC (clone 266), and CD146-PE (clone P1H12). 7AAD$^-$ CD45$^-$ CD31$^-$ CD71$^-$ cells were isolated according to CD105 and CD146 expression into CD105$^+$ CD146$^+$, CD105$^+$ CD146$^-$ and CD105$^-$ CD146$^-$ cells. For other experiments, the filters used to trap bone spicules and cell aggregates were carefully and aseptically washed with cold PBS several times. Cells were recovered by centrifugation and erythrocytes were lysed with 0.8% NH_4Cl. After a wash and centrifugation, the pellet was enzymatically dissociated in a solution containing 0.25% type I collagenase and 20% fetal bovine serum (FBS) in PBS (StemCell Technologies) for 30 min at 37°C, with mechanical agitation every 10 min.

Human fetal BM samples were obtained from Leiden University Medical Center (The Netherlands) under a protocol approved by the ethics committee of that institution. Fetal BM samples were mechanically dispersed and the mononuclear cells were isolated by Ficoll gradient, frozen, and kept in liquid nitrogen. Cells were thawed, washed with PBS once, and stained with antibodies for immunomagnetic enrichment using anti-CD45 magnetic beads (Miltenyi Biotec) according to the manufacturer's recommendations.

For sphere formation, sorted cells were plated at low density (<1,000 cells/cm^2) or by single-cell deposition in ultralow-adherence 35 mm dishes (StemCell Technologies). The growth medium for both CEE and HS spheres contained 0.1 mM β-mercaptoethanol; 1% nonessential amino acids (Sigma); 1% N2 and 2% B27 supplements (Invitrogen); recombinant human fibroblast growth factor (FGF)-basic, recombinant human epidermal growth factor (EGF), recombinant human platelet-derived growth factor (PDGF-AB), recombinant human oncostatin M (227 aa OSM, 20 ng/ml) and recombinant human IGF-1 (40 ng/ml; Peprotech) in Dulbecco's modified Eagle's medium (DMEM)/F12 (1:1) / human endothelial (1:2) serum-free medium (Invitrogen). CEE medium was supplemented with 15% CEE prepared as described previously (Pajtler et al., 2010; Stemple and Anderson, 1992), and HS medium was instead supplemented with 10% HS. The cultures were kept at 37°C with 5% CO_2, 20% O_2 in a water-jacketed incubator and left untouched for 1 week to prevent cell aggregation. Afterward, half-medium changes were performed twice a week. For passage, spheres were enzymatically dissociated in 100 μl of a solution containing 0.25% type I collagenase and 20% FBS in PBS (StemCell Technologies) for 30 min at 37°C, with mechanical dispersion every 10 min. Cells were washed with PBS once and replated with mesensphere medium in ultralow-adherence 35 mm dishes (StemCell Technologies) at 37°C in a water-jacketed incubator with 5% CO_2 and 20% O_2.

Human CD34$^+$ cells pooled from cord blood samples were purchased (StemCell Technologies) or isolated as follows: Cord blood samples were obtained in accordance with procedures approved by the institutional ethics committee. Two to three cord blood units were pooled and erythrocytes were removed by Ficoll-Paque density gradient centrifugation. CD34$^+$ cells were isolated by magnetic cell selection using anti-hCD34 magnetic microbeads (Miltenyi) and frozen immediately after purification. Cord blood CD34$^+$ cells were cultured as previously described (Zhang et al., 2006) in StemSpan serum-free medium (StemCell Technologies) supplemented with 10 μg/ml heparin (Sigma), recombinant human stem cell factor, recombinant human FGF-1 (10 ng/ml), recombinant human thrombopoietin (20 ng/ml; Peprotech), and 1% penicillin-streptomycin (Invitrogen) at 37°C in a water-jacketed incubator with 5% CO_2. Culture dishes were diluted 1:1 with fresh medium two to three times a week to maintain cell density. Spheres were directly added to the culture dishes or placed in the upper chamber of a 0.2 μm pore polycarbonate transwell (Corning) in the same medium. Spheres were cocultured with CD34$^+$ cells at a starting ratio of 1:1,000.

Immunostaining and Histology

Human BM biopsies were obtained in the Clínic Hospital (Barcelona, Spain) from healthy donors with their written consent. The biopsy specimens were embedded in paraffin, sectioned with a microtome, and mounted onto slides. After deparaffinization with xylol, the sections were rehydrated and washed with PBS. Sections were washed and blocked with blocking buffer (PBS with 0.1% Triton X-100, 10% donkey serum) for 30 min and incubated overnight at 4°C with primary antibodies in blocking buffer (rabbit anti-human Nestin [Millipore 1:200], goat anti-human endoglin [R&D 1:20] or control rabbit or goat immunoglobulin G [IgG] at the same concentrations). The samples were washed in PBS several times and incubated with species-specific fluorescent secondary antibodies (Alexa 488-conjugated donkey anti-rabbit IgG [Invitrogen] and Cy3-conjugated donkey anti-goat IgG [Jackson Laboratories]). The samples were then washed in PBS with 0.1% Triton X-100 and mounted (Vectashield fluorescent mounting medium with DAPI; Vector Labs). Images were captured using a confocal microscope (Sp5; Leica) with acquisition software (LAS AF; Leica). For histological analysis, human mesenspheres were fixed in suspension with 2% paraformaldehyde in PBS and embedded in paraffin for sectioning. Microtome sections were processed with routine hematoxylin and eosin (H&E) staining and images were acquired using a Zeiss Axiovert 200 microscope.

In Vitro Differentiation

Osteoblastic differentiation was induced by culturing the cells for 4 weeks with 50 μg/ml L-ascorbic acid 2-phosphate, 10 mM glycerophosphate (Sigma), and 15% FBS in α-MEM with 1% penicillin-streptomycin (Invitrogen). Adipocyte differentiation was induced with 1 μM dexamethasone, 10 μg/ml insulin (Sigma), and 10% FBS in α-MEM with 1% penicillin-streptomycin (Invitrogen). Chondrogenic differentiation was induced in cell pellets with 10^{-7} M dexamethasone, 10^{-4} M L-ascorbic acid 2-phosphate, 1 mM sodium pyruvate, nonessential amino acids, 1× SITE+3 supplement (1 mg/ml human insulin, 0.55 mg/ml human transferrin, 0.5 μg/ml sodium selenite, 0.2 mg/ml ethanolamine, 470 μg/ml linoleic acid, 470 μg/ml oleic acid, and 50 mg/ml bovine serum albumin; Sigma) and 10 ng/ml TGF-β3 (Peprotech) in DMEM with 1% penicillin-streptomycin (Invitrogen) over 2–4 weeks. All cultures were maintained with 5% CO_2 in a water-jacketed incubator at 37°C, and half-medium changes were performed twice a week. To assess in vitro differentiation into mesenchymal lineages, cells were briefly washed with PBS and fixed for 10 min with 2% paraformaldehyde in PBS (Sigma). For the detection of alkaline phosphatase activity, cells were washed twice with PBS and incubated for 20 min at room temperature with 50 μg/ml Naphthol AS-MX phosphate, 0.5% N,N-Dimethylformamide, and 0.6 mg/ml Fast Red Violet LB in 0.1 M Tris-HCl, pH 8.9. Alizarin red staining of calcium deposits was performed in fixed cultures washed with distilled water and incubated with 2% alizarin red for 5 min, followed by washes in distilled water. Adipocytes were stained with oil red O as follows: cells were washed with 60% isopropanol and allowed to dry completely. An oil red working solution was prepared as a 6:4 dilution in distilled water of a 0.35 g/ml oil red O solution in isopropanol (Sigma) and filtered 20 min later. Cells were incubated for 10 min with oil red working solution and rinsed 4 times. To stain mucopolysaccharides associated with chondrocytic differentiation, fixed cultures and cell pellets were incubated for 30 min at room temperature with 1% Alcian blue 8GX (Sigma) in 3% acetic acid, pH 2.5, and rinsed four times. For toluidine blue staining of chondrocytes, fixed spheres or their rehydrated paraffin sections were incubated in 1% toluidine blue (Amresco) in 1% sodium tetraborate decahydrate (Sigma) for 5 or 2 min, respectively, and washed afterward.

RNA Isolation and Real-Time Quantitative RT-PCR

RNA isolation was performed using the Dynabeads mRNA DIRECT Micro Kit (Invitrogen). RT was performed using the Reverse Transcription System (Promega) according to the manufacturer's recommendations. Real-time quantitative RT-PCR (qRT-PCR) was performed as previously described (Méndez-Ferrer et al., 2008). The expression level of each gene was determined by using the relative standard curve method. Briefly, a standard curve was obtained by serial dilutions of a human reference total RNA (Clontech). The expression level of each gene was calculated by interpolation from the standard curve. All values were normalized with glyceraldehyde 3-phosphate dehydrogenase (GAPDH) as the endogenous control. The sequences of the oligonucleotides used for PCR are provided in Table S3.

In Vivo Transplantation and Hematopoietic Human Chimerism in Immunodeficient Mice

Freshly thawed 10^4 cord blood $CD34^+$ cells or their cultured progeny were washed and resuspended in 100 μl PBS and i.v. injected, retro-orbitally or through the tail vein, into immunodeficient mice previously anesthetized with sevoflurane. Two months after transplantation, the femora was crushed in cold PBS and the BM was harvested and analyzed by FACS (without lysing red blood cells) to detect the presence of human hematopoietic cells in the BM of the recipient mice.

In Vivo Transplantation of Human Mesenspheres in Subcutaneous Ossicles in Immunodeficient Mice

Ceramic porous cubes (~3 mm^3) composed of 65% calcium phosphate hydroxyapatite and 35% tricalcium phosphate (Ceraform) were washed with distilled water twice to discard small detached fragments, autoclaved, and coated with 0.1 mg/ml fibronectin from bovine plasma (Sigma). To eliminate the air contained in the cubes and ensure proper coating of the pores, the ossicles were placed in a FACS tube containing the fibronectin solution and agitated for 1 min while negative pressure was applied by suction with a 60 ml syringe and a 21 gauge needle through the tube cap. The cap was replaced by a new one and the procedure was repeated once. Fibronectin-coated ossicles were allowed to dry overnight in a laminar flow hood. Single human mesenspheres were gently deposited onto the ossicles and allowed to attach for 24 hr in the incubator. The ossicles were implanted s.c. under the dorsal skin of 6- to 12-week-old anesthetized recipient NOD/SCID mice. Two months later, the ossicles were harvested and enzymatically dissociated in a solution containing 0.25% type I collagenase and 20% FBS in PBS (StemCell Technologies) for 60 min at 37°C, with mechanical agitation every 10 min. The recovered cells were analyzed by FACS.

Detailed methods for the secretome proteomics are available in the Extended Experimental Procedures.

SUPPLEMENTAL INFORMATION

Supplemental Information includes Extended Experimental Procedures, five figures, and three tables and can be found with this article online at http://dx.doi.org/10.1016/j.celrep.2013.03.041.

LICENSING INFORMATION

ACKNOWLEDGMENTS

We thank M. García-Fernández for invaluable support and helpful suggestions regarding the manuscript, Centro de Transfusión de la Comunidad de Madrid for providing cord blood, M. Ruiz and M. Sánchez for providing HS, J.M. Ligos for help with flow cytometry, R.B. Doohan for help with histology, G.E. Enikolopov for providing *Nestin-Gfp* mice, G. Giovinazzo for providing NOD/SCID mice, C. Heeschen for providing NSG mice, E. Calvo and E. Bonzón-Kulichenko for advice on proteomics, and Y. Torres and L. Amleto for help with cell culture and staining. This work was supported by the Fundación Centro Nacional de Investigaciones Cardiovasculares Carlos III, the Spanish Ministry of Economy and Competitiveness (SAF2011-30308 grant to S.M.-F., Ramón y Cajal Program grants RYC-2011-09209 to J.I., RYC-2011-09726 to A.S.-A., RYC-2009-04703 to S.M.-F., and BIO2009-07990 to J.V.); the Marie Curie Career Integration Program (FP7-PEOPLE-2011-RG-294262 to S.M.-F. and FP7-PEOPLE-2011-RG-294096 to A.S.-A.); Institute of Health Carlos III (RD06/0014/0030 to J.V. and PI11/01090 and RD06/0020/0012 to A.U.-I.); Consejería de Salud of Junta de Andalucía (PI0079 to A.U.-I); the Swedish Research Council, Swedish Cancer Foundation, and Swedish Childhood Cancer Foundation (grants to S.S.); and ConSEPOC-Comunidad de Madrid (S2010/BMD-2542 to S.M.-F.). J.I. was the recipient of a fellowship from the Spanish Ministry of Education. A.S.-A. received a research award from the European Hematology Association. S.M.-F. is supported in part by an International Early Career Scientist grant from the Howard Hughes Medical Institute.

Received: May 31, 2012
Revised: February 28, 2013
Accepted: March 27, 2013
Published: April 25, 2013

REFERENCES

Aslan, H., Zilberman, Y., Kandel, L., Liebergall, M., Oskouian, R.J., Gazit, D., and Gazit, Z. (2006). Osteogenic differentiation of noncultured immunoisolated bone marrow-derived CD105+ cells. Stem Cells *24*, 1728–1737.

Baksh, D., Davies, J.E., and Zandstra, P.W. (2003). Adult human bone marrow-derived mesenchymal progenitor cells are capable of adhesion-independent survival and expansion. Exp. Hematol. *31*, 723–732.

Boitano, A.E., Wang, J., Romeo, R., Bouchez, L.C., Parker, A.E., Sutton, S.E., Walker, J.R., Flaveny, C.A., Perdew, G.H., Denison, M.S., et al. (2010). Aryl hydrocarbon receptor antagonists promote the expansion of human hematopoietic stem cells. Science *329*, 1345–1348.

Bonzon-Kulichenko, E., Martínez-Martínez, S., Trevisan-Herraz, M., Navarro, P., Redondo, J.M., and Vázquez, J. (2011). Quantitative in-depth analysis of the dynamic secretome of activated Jurkat T-cells. J. Proteomics *75*, 561–571.

Breems, D.A., Blokland, E.A., and Ploemacher, R.E. (1997). Stroma-conditioned media improve expansion of human primitive hematopoietic stem cells and progenitor cells. Leukemia *11*, 142–150.

Broxmeyer, H.E. (2011). Insights into the biology of cord blood stem/progenitor cells. Cell Prolif. *44*(*Suppl 1*), 55–59.

Campbell, T.B., Hangoc, G., Liu, Y., Pollok, K., and Broxmeyer, H.E. (2007). Inhibition of CD26 in human cord blood CD34+ cells enhances their engraftment of nonobese diabetic/severe combined immunodeficiency mice. Stem Cells Dev. *16*, 347–354.

Christopherson, K.W., 2nd, Paganessi, L.A., Napier, S., and Porecha, N.K. (2007). CD26 inhibition on CD34+ or lineage- human umbilical cord blood donor hematopoietic stem cells/hematopoietic progenitor cells improves long-term engraftment into NOD/SCID/Beta2null immunodeficient mice. Stem Cells Dev. *16*, 355–360.

de Lima, M., McNiece, I., Robinson, S.N., Munsell, M., Eapen, M., Horowitz, M., Alousi, A., Saliba, R., McMannis, J.D., Kaur, I., et al. (2012). Cord-blood engraftment with ex vivo mesenchymal-cell coculture. N. Engl. J. Med. *367*, 2305–2315.

Delaney, C., Heimfeld, S., Brashem-Stein, C., Voorhies, H., Manger, R.L., and Bernstein, I.D. (2010). Notch-mediated expansion of human cord blood progenitor cells capable of rapid myeloid reconstitution. Nat. Med. *16*, 232–236.

Di Maggio, N., Mehrkens, A., Papadimitropoulos, A., Schaeren, S., Heberer, M., Banfi, A., and Martin, I. (2012). Fibroblast growth factor-2 maintains a niche-dependent population of self-renewing highly potent non-adherent mesenchymal progenitors through FGFR2c. Stem Cells *30*, 1455–1464.

Ding, L., Saunders, T.L., Enikolopov, G., and Morrison, S.J. (2012). Endothelial and perivascular cells maintain haematopoietic stem cells. Nature *481*, 457–462.

Ferraro, F., Lymperi, S., Méndez-Ferrer, S., Saez, B., Spencer, J.A., Yeap, B.Y., Masselli, E., Graiani, G., Prezioso, L., Rizzini, E.L., et al. (2011). Diabetes impairs hematopoietic stem cell mobilization by altering niche function. Sci. Transl. Med. *3*, 104ra101.

Friedenstein, A.J., Chailakhjan, R.K., and Lalykina, K.S. (1970). The development of fibroblast colonies in monolayer cultures of guinea-pig bone marrow and spleen cells. Cell Tissue Kinet. *3*, 393–403.

Goessling, W., Allen, R.S., Guan, X., Jin, P., Uchida, N., Dovey, M., Harris, J.M., Metzger, M.E., Bonifacino, A.C., Stroncek, D., et al. (2011). Prostaglandin E2 enhances human cord blood stem cell xenotransplants and shows long-term safety in preclinical nonhuman primate transplant models. Cell Stem Cell *8*, 445–458.

Harvey, K., and Dzierzak, E. (2004). Cell-cell contact and anatomical compatibility in stromal cell-mediated HSC support during development. Stem Cells *22*, 253–258.

Hoggatt, J., Singh, P., Sampath, J., and Pelus, L.M. (2009). Prostaglandin E2 enhances hematopoietic stem cell homing, survival, and proliferation. Blood *113*, 5444–5455.

Kawada, H., Ando, K., Tsuji, T., Shimakura, Y., Nakamura, Y., Chargui, J., Hagihara, M., Itagaki, H., Shimizu, T., Inokuchi, S., et al. (1999). Rapid ex vivo expansion of human umbilical cord hematopoietic progenitors using a novel culture system. Exp. Hematol. *27*, 904–915.

Larsson, J., and Karlsson, S. (2005). The role of Smad signaling in hematopoiesis. Oncogene *24*, 5676–5692.

Méndez-Ferrer, S., Lucas, D., Battista, M., and Frenette, P.S. (2008). Haematopoietic stem cell release is regulated by circadian oscillations. Nature *452*, 442–447.

Méndez-Ferrer, S., Michurina, T.V., Ferraro, F., Mazloom, A.R., Macarthur, B.D., Lira, S.A., Scadden, D.T., Ma'ayan, A., Enikolopov, G.N., and Frenette, P.S. (2010). Mesenchymal and haematopoietic stem cells form a unique bone marrow niche. Nature *466*, 829–834.

Mercier, F.E., Ragu, C., and Scadden, D.T. (2012). The bone marrow at the crossroads of blood and immunity. Nat. Rev. Immunol. *12*, 49–60.

Mignone, J.L., Kukekov, V., Chiang, A.S., Steindler, D., and Enikolopov, G. (2004). Neural stem and progenitor cells in nestin-GFP transgenic mice. J. Comp. Neurol. *469*, 311–324.

Nilsson, S.K., Johnston, H.M., Whitty, G.A., Williams, B., Webb, R.J., Denhardt, D.T., Bertoncello, I., Bendall, L.J., Simmons, P.J., and Haylock, D.N. (2005). Osteopontin, a key component of the hematopoietic stem cell niche and regulator of primitive hematopoietic progenitor cells. Blood *106*, 1232–1239.

North, T.E., Goessling, W., Walkley, C.R., Lengerke, C., Kopani, K.R., Lord, A.M., Weber, G.J., Bowman, T.V., Jang, I.H., Grosser, T., et al. (2007). Prostaglandin E2 regulates vertebrate haematopoietic stem cell homeostasis. Nature *447*, 1007–1011.

Notta, F., Doulatov, S., Laurenti, E., Poeppl, A., Jurisica, I., and Dick, J.E. (2011). Isolation of single human hematopoietic stem cells capable of long-term multilineage engraftment. Science *333*, 218–221.

Omatsu, Y., Sugiyama, T., Kohara, H., Kondoh, G., Fujii, N., Kohno, K., and Nagasawa, T. (2010). The essential functions of adipo-osteogenic progenitors as the hematopoietic stem and progenitor cell niche. Immunity *33*, 387–399.

Pajtler, K., Bohrer, A., Maurer, J., Schorle, H., Schramm, A., Eggert, A., and Schulte, J.H. (2010). Production of chick embryo extract for the cultivation of murine neural crest stem cells. J. Vis. Exp. *27*, pii: 2380.

Robinson, S.N., Simmons, P.J., Thomas, M.W., Brouard, N., Javni, J.A., Trilok, S., Shim, J.S., Yang, H., Steiner, D., Decker, W.K., et al. (2012). Ex vivo fucosylation improves human cord blood engraftment in NOD-SCID IL-2Rγ(null) mice. Exp. Hematol. *40*, 445–456.

Sacchetti, B., Funari, A., Michienzi, S., Di Cesare, S., Piersanti, S., Saggio, I., Tagliafico, E., Ferrari, S., Robey, P.G., Riminucci, M., and Bianco, P. (2007). Self-renewing osteoprogenitors in bone marrow sinusoids can organize a hematopoietic microenvironment. Cell *131*, 324–336.

Sangeetha, V.M., Kale, V.P., and Limaye, L.S. (2010). Expansion of cord blood CD34 cells in presence of zVADfmk and zLLYfmk improved their in vitro functionality and in vivo engraftment in NOD/SCID mouse. PLoS ONE *5*, e12221.

Schofield, R. (1978). The relationship between the spleen colony-forming cell and the haemopoietic stem cell. Blood Cells *4*, 7–25.

Sharma, M.B., Limaye, L.S., and Kale, V.P. (2011). Mimicking the functional hematopoietic stem cell niche in vitro: recapitulation of marrow physiology by hydrogel-based three-dimensional cultures of mesenchymal stromal cells. Haematologica *97*, 651–660.

Stemple, D.L., and Anderson, D.J. (1992). Isolation of a stem cell for neurons and glia from the mammalian neural crest. Cell *71*, 973–985.

Stier, S., Ko, Y., Forkert, R., Lutz, C., Neuhaus, T., Grünewald, E., Cheng, T., Dombkowski, D., Calvi, L.M., Rittling, S.R., and Scadden, D.T. (2005). Osteopontin is a hematopoietic stem cell niche component that negatively regulates stem cell pool size. J. Exp. Med. *201*, 1781–1791.

Thiemann, F.T., Moore, K.A., Smogorzewska, E.M., Lemischka, I.R., and Crooks, G.M. (1998). The murine stromal cell line AFT024 acts specifically on human CD34+CD38- progenitors to maintain primitive function and immunophenotype in vitro. Exp. Hematol. *26*, 612–619.

Tormin, A., Li, O., Brune, J.C., Walsh, S., Schütz, B., Ehinger, M., Ditzel, N., Kassem, M., and Scheding, S. (2011). CD146 expression on primary nonhematopoietic bone marrow stem cells is correlated with in situ localization. Blood *117*, 5067–5077.

Urbano-Ispizua, A., Rozman, C., Pimentel, P., Solano, C., de la Rubia, J., Brunet, S., Pérez-Oteiza, J., Ferrá, C., Zuazu, J., Caballero, D., et al.; Spanish Group for Allogenic Peripheral Blood Transplantation. (2001). The number of donor CD3(+) cells is the most important factor for graft failure after allogeneic transplantation of CD34(+) selected cells from peripheral blood from HLA-identical siblings. Blood *97*, 383–387.

Verfaillie, C.M. (1992). Direct contact between human primitive hematopoietic progenitors and bone marrow stroma is not required for long-term in vitro hematopoiesis. Blood *79*, 2821–2826.

Zhang, C.C., Kaba, M., Ge, G., Xie, K., Tong, W., Hug, C., and Lodish, H.F. (2006). Angiopoietin-like proteins stimulate ex vivo expansion of hematopoietic stem cells. Nat. Med. *12*, 240–245.

Zhang, C.C., Kaba, M., Iizuka, S., Huynh, H., and Lodish, H.F. (2008). Angiopoietin-like 5 and IGFBP2 stimulate ex vivo expansion of human cord blood hematopoietic stem cells as assayed by NOD/SCID transplantation. Blood *111*, 3415–3423.

Cell PRESS
Open ACCESS

EXTENDED EXPERIMENTAL PROCEDURES

Secretome Proteomics

Human mesenspheres propagated with medium containing HS or CEE, prepared as previously described (Pajtler et al., 2010; Stemple and Anderson, 1992), were washed four times with PBS and incubated for 72 hr in serum-free, phenol-red free minimal essential medium-alpha (Invitrogen) supplemented with 0.1 mM β-mercaptoethanol, 1% non-essential aminoacids (Sigma), recombinant human fibroblast growth factor (FGF)-basic, recombinant human epidermal growth factor (EGF), recombinant human platelet-derived growth factor (PDGF-AB), recombinant human oncostatin M (227 aa OSM; 20 ng/ml) and recombinant human insulin-like growth factor-1 (IGF-1; 40 ng/ml; Peprotech) to collect supernatants suitable for proteomics analyses. Supernatants were centrifuged at 1300 rpm for 5 min to discard cells. Protein in-gel digestion of the supernatants was performed as previously described (Bonzon-Kulichenko et al., 2011b), with some modifications. Briefly, the supernatants were run by conventional SDS-PAGE until the front entered 3 mm into the resolving gel. The protein band containing the whole proteome was visualized by Coomassie staining, excised, cut into cubes, subjected to reduction and alkylation, and digested overnight at 37°C with 60 ng/μl trypsin at 10:1 protein:trypsin (w/w) ratio in 50 mM ammonium bicarbonate, pH 8.8 containing 10% ACN. The resulting tryptic peptides from each proteome were extracted by 1h-incubation in 12 mM ammonium bicarbonate, pH 8.8. TFA was added to a final concentration of 1% and the peptides were finally desalted onto C18 Oasis cartridges and dried-down. Dried peptides were subjected to differential $^{16}O/^{18}O$ labeling, as previously described (Ramos-Fernández et al., 2007). Tryptic peptides were analyzed by LC-MS/MS using a C-18 reversed phase nano-column (75 μm I.D. x 25 cm, 3 μm particle size, Acclaim PepMap 100 C18, Thermo-Fisher) and analyzed in a continuous acetonitrile gradient consisting of 0%–30% B in 145 min, 30%–43% in 5 min and 43%–90% B in 1 min (A = 0.5% formic acid; B = 95% acetonitrile, 0.5% formic acid). A flow rate of *ca.* 300 nL/min was used to elute peptides from the reverse phase nano-column to an emitter nanospray needle for real time ionization and peptide fragmentation on an orbital ion trap mass spectrometer (LTQ-Orbitrap XL, Thermo-Fisher). An enhanced resolution spectrum (resolution = 60000) followed by the MS/MS spectra from the five most intense parent ions were analyzed during the chromatographic run (180 min). Dynamic exclusion was set at 0.5 min. In order to increase secretome coverage, tryptic peptides were fractionated by cation exchange chromatography into four fractions, which were analyzed by using an Orbitrap Elite mass spectrometer (Thermo-Fisher). For peptide identification, all spectra were analyzed with Proteome Discoverer (version 1.3.0.339, Thermo Fisher Scientific), using a Uniprot database containing all human and chicken protein sequences (November 23, 2011). For database searching, parameters were selected as follows: trypsin digestion with 2 maximum missed cleavage sites, precursor mass tolerance of 20 ppm, fragment mass tolerance of 1200 mmu, carbamidomethyl cysteine as fixed modification, and methionine oxidation and ^{18}O labeling in lysine and arginine residues as dynamic modifications. Peptide identification was validated using the probability ratio method (Martínez-Bartolomé et al., 2008) and FDR were calculated using inverted databases and the refined method (Navarro and Vázquez, 2009). ^{18}O Labeling efficiency was controlled as described (Ramos-Fernández et al., 2007). Potentially secreted proteins were determined and quantitated as previously described (Bonzon-Kulichenko et al., 2011a). Statistical analysis of quantitative ^{18}O data was performed on the basis of a validated random-effects model that includes four different sources of variance at the spectrum-fitting, scan, peptide and protein levels (Jorge et al., 2009). For functional protein analysis, protein $\log_2$-ratios standardized according to their estimated variances (Zq values) were classified in terms of the Gene Ontology Biological Process and Cellular Component, KEGG and Reactome, by using an in-house program. The significance of enrichment for different categories was assessed by Student's t test, as previously described (Bonzon-Kulichenko et al., 2011a).

SUPPLEMENTAL REFERENCES

Bonzon-Kulichenko, E., Martínez-Martínez, S., Trevisan-Herraz, M., Navarro, P., Redondo, J.M., and Vázquez, J. (2011a). Quantitative in-depth analysis of the dynamic secretome of activated Jurkat T-cells. J. Proteomics *75*, 561–571.

Bonzon-Kulichenko, E., Perez-Hernandez, D., Nunez, E., Martinez-Acedo, P., Navarro, P., Trevisan-Herraz, M., Ramos Mdel, C., Sierra, S., Martinez-Martinez, S., Ruiz-Meana, M., et al. (2011b). A robust method for quantitative high-throughput analysis of proteomes by 18O labeling. Mol. Cell. Proteomics *10*, M110.003335.

Jorge, I., Navarro, P., Martínez-Acedo, P., Núñez, E., Serrano, H., Alfranca, A., Redondo, J.M., and Vázquez, J. (2009). Statistical model to analyze quantitative proteomics data obtained by 18O/16O labeling and linear ion trap mass spectrometry: application to the study of vascular endothelial growth factor-induced angiogenesis in endothelial cells. Mol. Cell. Proteomics *8*, 1130–1149.

Martínez-Bartolomé, S., Navarro, P., Martín-Maroto, F., López-Ferrer, D., Ramos-Fernández, A., Villar, M., García-Ruiz, J.P., and Vázquez, J. (2008). Properties of average score distributions of SEQUEST: the probability ratio method. Mol. Cell. Proteomics *7*, 1135–1145.

Navarro, P., and Vázquez, J. (2009). A refined method to calculate false discovery rates for peptide identification using decoy databases. J. Proteome Res. *8*, 1792–1796.

Ramos-Fernández, A., López-Ferrer, D., and Vázquez, J. (2007). Improved method for differential expression proteomics using trypsin-catalyzed 18O labeling with a correction for labeling efficiency. Mol. Cell. Proteomics *6*, 1274–1286.

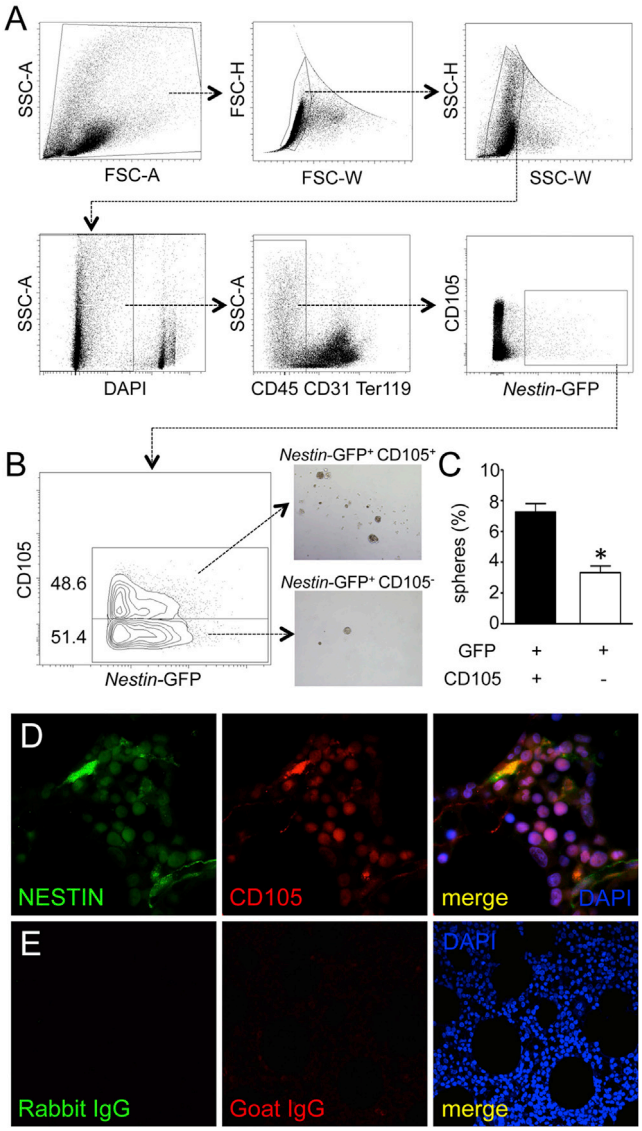

Figure S1. Expression of Endoglin in nestin$^+$ Mesensphere-Forming Cells, Related to Figure 1

(A–C) Murine BM mesenspheres are enriched within the CD105$^+$ subset of *Nestin*-GFP$^+$ cells.

(A) Representative FACS diagrams of CD45$^-$ CD31$^-$ Ter119$^-$ GFP$^+$ cells isolated from the BM of *Nestin-Gfp* transgenic mice showing GFP and CD105 expression.

(B and C) Representative examples of (B) mesenspheres and (C) sphere-forming efficiency of CD45$^-$ CD31$^-$ Ter119$^-$ *Nestin*-GFP$^+$ CD105$^+$ and CD45$^-$ CD31$^-$ Ter119$^-$ *Nestin*-GFP$^+$ CD105$^-$ cells; n = 3; *$p < 0.05$; unpaired two-tailed t test. Error bars indicate SEM.

(D and E) Coexpression of nestin and endoglin in human BM cells. Confocal projections of z-stacks of 10 μm paraffin sections of healthy human BM biopsies stained using (D) anti-nestin (green), anti-CD105 (red), or (E) control isotype antibodies. Nuclei were counterstained with DAPI (blue).

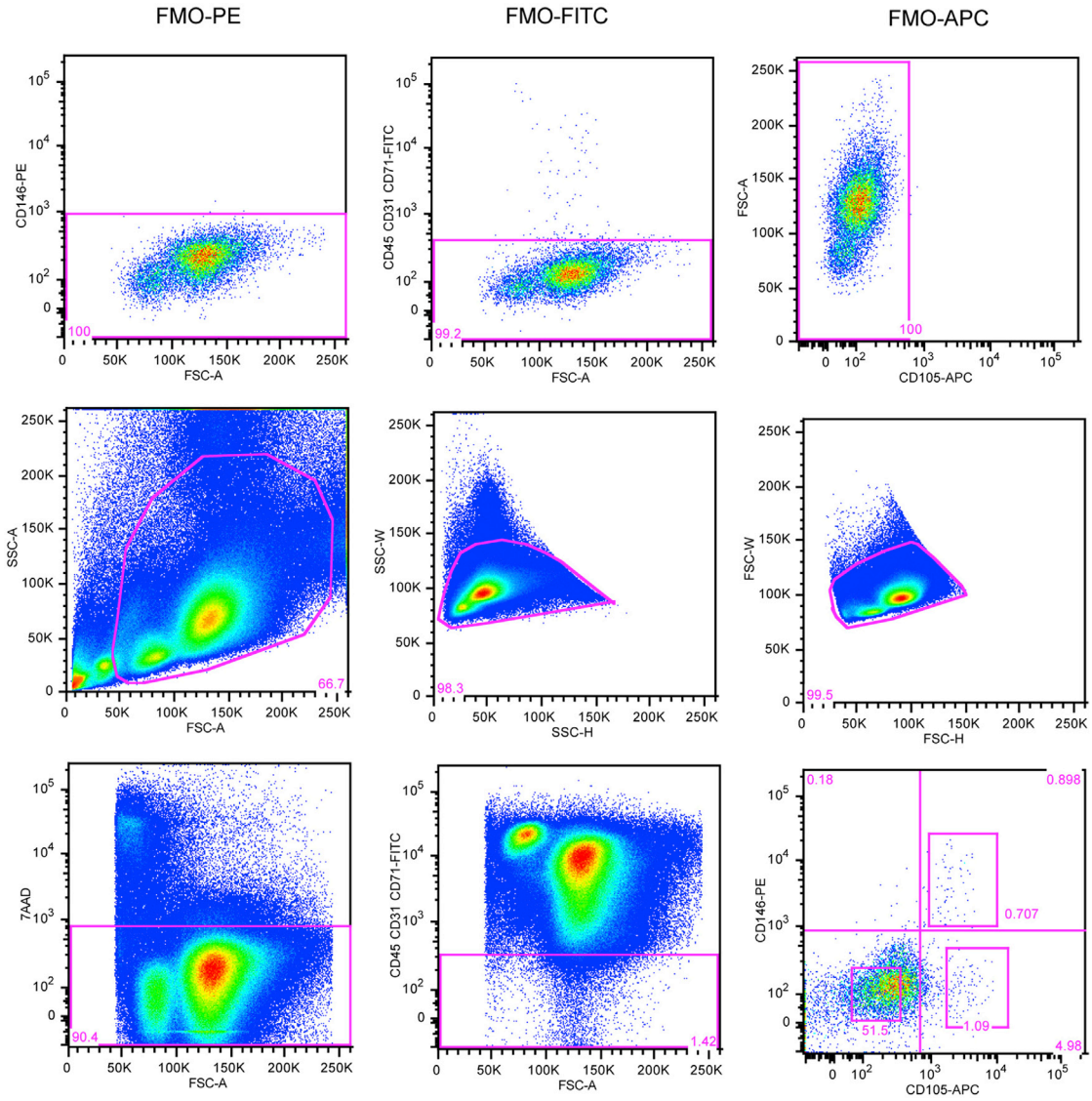

Figure S2. Human BM Mesenspheres Are Derived from CD45$^-$ CD31$^-$ CD71$^-$ CD105$^+$ CD146$^+$ Cells, Related to Figure 2

Isolation protocol for human BMSCs. Human BM mononuclear cells were enriched using the RosetteSep kit (StemCell Technologies). Representative FACS diagrams showing the isolation protocol. Upper panel, control stainings with fluorochrome-conjugated isotype antibodies and gating strategy. Medium panel, population gating by cell size and exclusion of doublets. Lower panel, cells were stained with 7-AAD solution (Sigma) and the following mouse anti-human antibodies (BD PharMingen): CD31-FITC (clone WM59), CD45-FITC (clone 2D1), CD71-FITC (clone M-A712), CD105-APC (clone 266) and CD146-PE (clone P1H12). 7AAD$^-$ CD45$^-$ CD31$^-$ CD71$^-$ cells were isolated according to CD105 and CD146 expression into CD105$^+$ CD146$^+$, CD105$^+$ CD146$^-$ and CD105$^-$ CD146$^-$ cells. The percentage of each population is indicated.

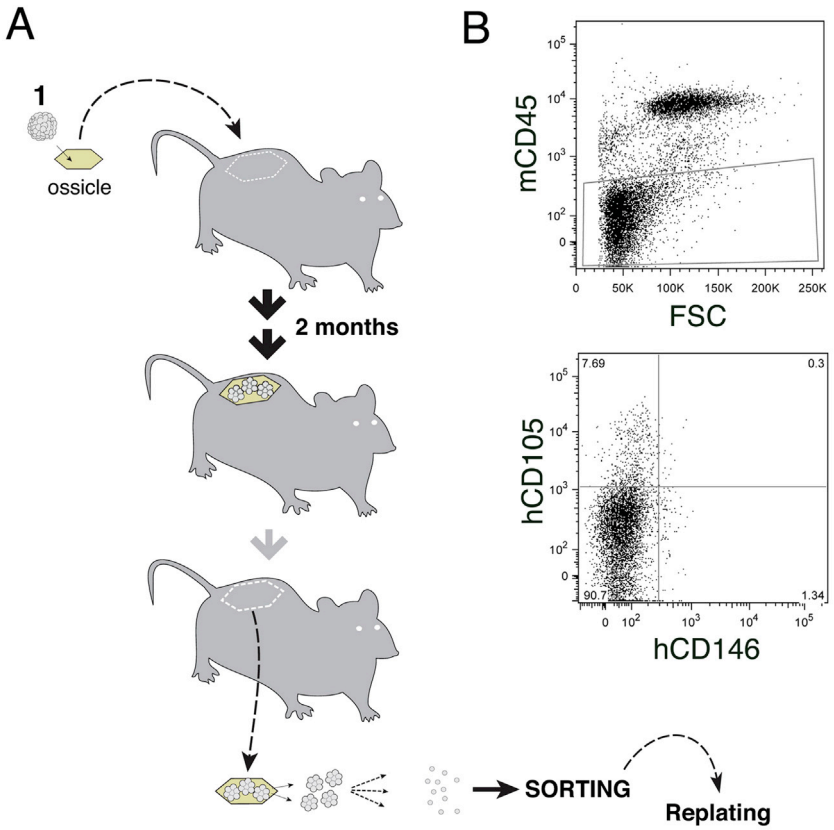

C

Efficiency of secondary sphere formation from ossicles loaded with human mesenspheres (%)		
hCD105$^+$	hCD146$^+$	hCD105$^-$ hCD146$^-$
32 (9/28) 11 (4/38)	47 (65/137) 5.5 (1/18) 10.5 (4/38)	0.08 (18/23,000) 0.47 (114/24,000)

Figure S3. In Vivo Transplantation and Recovery of Human BM Mesenspheres, Related to Figure 4

(A) Single human BM mesenspheres were allowed to attach to fibronectin-coated ceramic porous cubes composed of 65% calcium phosphate hydroxyapatite and 35% tricalcium phosphate (Ceraform) and subcutaneously implanted (1 sphere/ossicle) into NOD/SCID mice. The ossicles were recovered after 2 months and were enzymatically digested.

(B) Cells harvested from the ossicles were isolated by FACS according to mCD45, hCD105 and hCD146 expression and were replated in mesensphere-forming medium.

(C) Efficiency of secondary sphere formation from stromal hCD105$^+$, hCD146$^+$ and hCD105$^-$ hCD146$^-$ cells sorted from the ossicles.

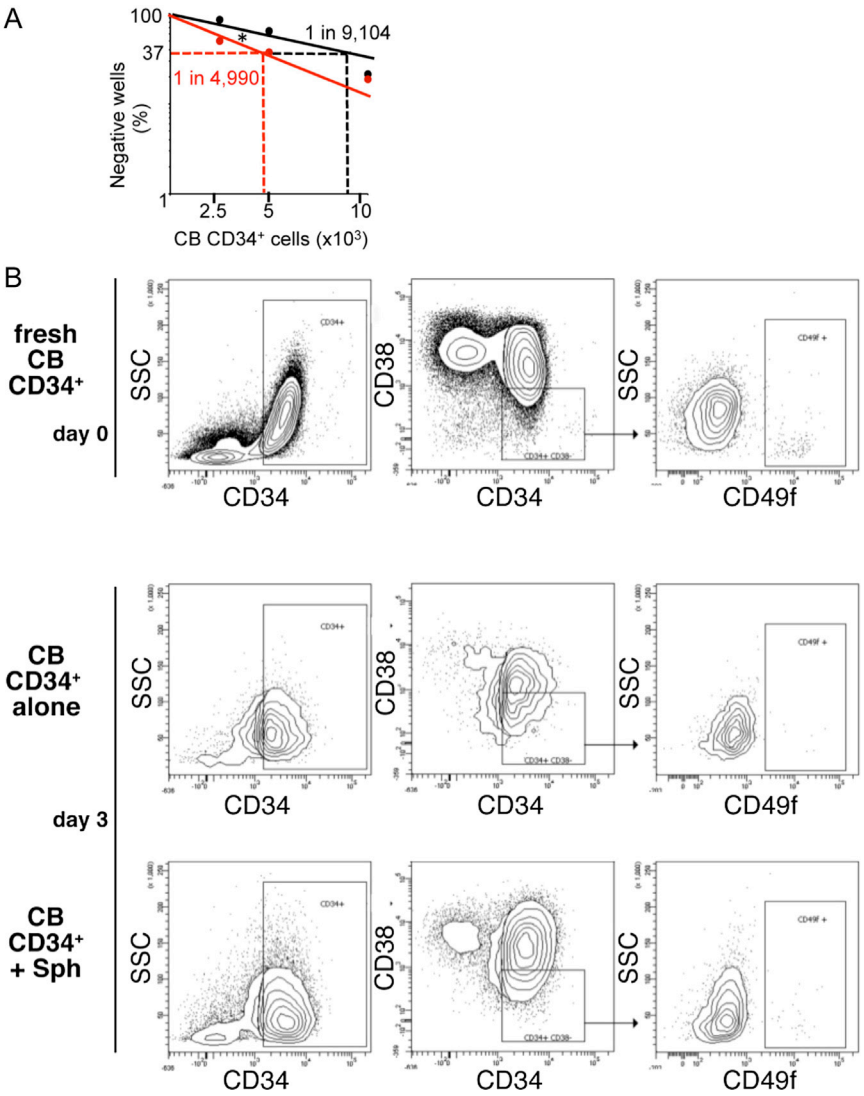

Figure S4. Human BM Mesenspheres Support Primitive Hematopoietic Progenitors, Related to Figures 5 and 6

(A) Coculture of ~100 fresh human primary BM mesenspheres with $2x10^5$ cord blood $CD34^+$ cells did not change the output cell yield but nearly doubled the number of primitive hematopoietic progenitors, measured using the long-term culture initiating cell assay (LTCIC). The percentage of culture dishes in each experimental group that failed to generate colony-forming units (CFU-C) is plotted against the number of test cord blood $CD34^+$ cells cultured alone (black) or in the presence of human BM mesenspheres (red); HSC frequencies are indicated; Pearson chi-square test; $^*p < 0.05$ (n = 4–6).

(B) Maintenance of cord blood primitive progenitor immunophenotype after coculture with human BM-derived mesenspheres. Fresh human umbilical cord blood was obtained and $CD34^+$ cells were enriched using CD34-positive selection kit (StemCell Technologies). CD34-enriched cells were analyzed for surface expression of CD34, CD38 and CD49f to assess the frequencies of the most primitive hematopoietic progenitors by immmunophenotype. The starting purity of CD34 cells at the beginning of the culture was 60%–70% (top panels). Purified cord blood $CD34^+$ cells were cocultured with or without human mesenspheres (lower panels "+Sph," and middle panels, "alone," respectively) at 37°C, 5% CO_2 in StemSpan Serum Free Medium (StemCell Technologies) supplemented with 100 ng/ml stem cell factor, 100 ng/ml FLT-3 ligand, 50 ng/ml thrombopoietin, 50 ng/ml IL-6 and 50 ng/ml IL-3. The expression of CD34, CD38 and CD49f was analyzed by FACS after 3 days in culture.

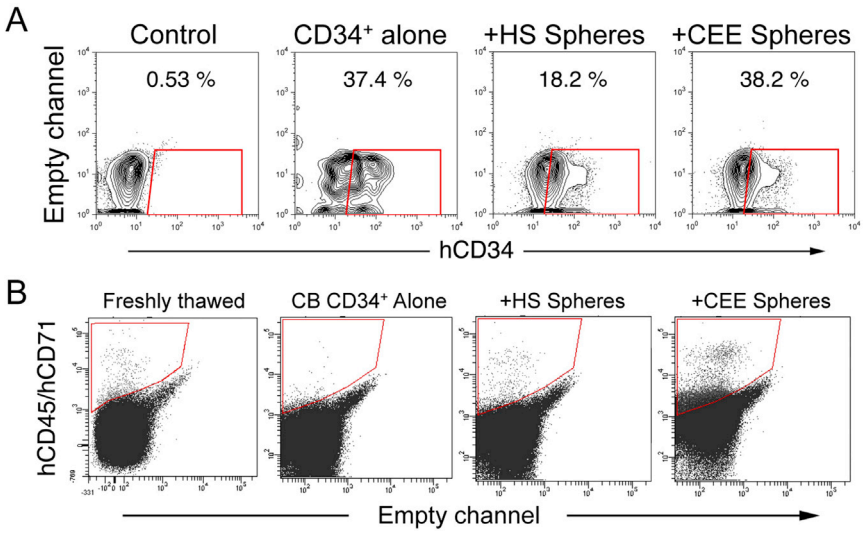

Figure S5. Human BM Mesenspheres Expand SCID-Repopulating Units, Related to Figures 5 and 6

Cord blood CD34$^+$ cells were cultured for 16 days in serum-free medium containing cytokines in the absence (alone) or presence of human BM mesenspheres previously expanded with chicken embryo extract (CEE) or human serum (HS).

(A) Representative flow diagrams of cultured viable cells stained with anti-hCD34 antibody (clone 581, BD PharMingen).

(B) Human chimerism in the BM of immunodeficient mice. Representative flow diagrams of viable cells in the BM of NOD/SCID mice two months after transplantation of 10^4 freshly thawed cord blood CD34$^+$ cells or their progeny after 16 days of culture with cytokine-supplemented serum-free medium alone or in the presence of HS or CEE spheres. Cells were stained with anti-hCD45 (clone HI30) and anti-hCD71 (clone M-A712) antibodies (BD PharMingen).